

## Preparation and characterization of a composite nanofiltration membrane from cyclen and trimesoyl chloride prepared by interfacial polymerization

Gui-E. Chen,<sup>1</sup> Yan-Jun Liu,<sup>1</sup> Zhen-Liang Xu,<sup>2</sup> Deng Hu,<sup>2</sup> Hui-Hong Huang,<sup>1</sup> Li Sun<sup>1</sup>

<sup>1</sup>School of Chemical and Environmental Engineering, Shanghai Institute of Technology, 100 Haiquan Road, Shanghai 201418, China

<sup>2</sup>Membrane Science and Engineering R&D Lab, State Key Laboratory of Chemical Engineering, Chemical Engineering Research Center, East China University of Science and Technology, 130 Meilong Road, Shanghai 200237, China

Correspondence to: Gui-E. Chen (E-mail: chenguie@sit.edu.cn)

**ABSTRACT:** A novel nanofiltration (NF) membrane was prepared with cyclen and trimesoyl chloride by interfacial polymerization on a poly(ether sulfone) ultrafiltration membrane with a molecular weight cutoff of 50,000 Da. The effects of the reaction time, monomer concentration, and heat-treatment temperature are discussed. The physicochemical properties and morphology of the prepared NF membrane were characterized by Fourier transform infrared spectroscopy–attenuated total reflectance, scanning electron microscopy, energy-dispersive spectrometry, and atomic force microscopy. The NF performances were evaluated with solutions of Na<sub>2</sub>SO<sub>4</sub>, MgSO<sub>4</sub>, Mg(NO<sub>3</sub>)<sub>2</sub>, and NaCl. The salt-rejection order of the prepared NF membrane was as follows: Na<sub>2</sub>SO<sub>4</sub> > MgSO<sub>4</sub> > Mg(NO<sub>3</sub>)<sub>2</sub> > NaCl. The resulting rejection of Na<sub>2</sub>SO<sub>4</sub> and PEG600 (polyethylene glycol with the average molecular weight of 600) were more than 90%, whereas that of NaCl was approximately 10%. After the addition of silica sol in the aqueous phase (silica sol concentration = 0.1% w/v), the salt rejection of the membrane changed slightly. However, the water flux was from 24.2 L·m<sup>-2</sup>·h<sup>-1</sup> (25°C, 0.6 MPa) up to 38.9 L·m<sup>-2</sup>·h<sup>-1</sup> (25°C, 0.6 MPa), and the resulting membrane exhibited excellent hydrophilicity. © 2015 Wiley Periodicals, Inc. *J. Appl. Polym. Sci.* **2015**, *132*, 42345.

**KEYWORDS:** membranes; polyamides; properties and characterization; surfaces and interfaces

Received 24 January 2015; accepted 10 April 2015

DOI: 10.1002/app.42345

### INTRODUCTION

Nanofiltration (NF) is a pressure-driven process positioned between ultrafiltration (UF) and reverse osmosis with respect to its flux and separation characteristics. This process is widely used to concentrate or separate aqueous solutions containing salts or organics. NF refers to a membrane process of rejecting solutes that are approximately 1 nm in size and with a molecular weight cutoff (MWCO) between 200 and 1000 Da. Hence, NF removes low-molecular weight organics and selects salts at lower pressures (typically from 0.5 to 1.5 MPa) than reverse osmosis does. In addition, NF is used at conditions in which a high salt rejection of reverse osmosis is not necessary.<sup>1–4</sup> With the advantages of low operation cost, relatively high flux, and high retention of multivalent ions or small organics, NF membranes have been widely used in wastewater treatment, pretreatment of seawater for desalination, pharmaceutical concentration, and dye removal. To separate or reject ions, the membrane not only needs nanosized pores structures but also surface charges. Given its huge economic benefits, the negatively

charged NF membrane has been paid more attention than the positively charged one. A reasonable adjustment of the NF surface porosity is very important in NF membrane preparation. Available techniques, such as the interfacial polymerization, photografting, dip coating, electron-beam irradiation, and plasma-initiated polymerization are commonly adopted to fabricate an ultrathin barrier layer upon a support membrane. Among these techniques, interfacial polymerization has gained considerable particular interests.<sup>5–7</sup> An advantage of the interfacial polymerization technique is the possibility of optimizing a thin layer for a particular function by regulating the reactant monomer structures, preparation conditions, and posttreatment.<sup>8–12</sup>

Through the interfacial polymerization of polymeric monomers, a series of negatively charged NF membranes have been prepared by the choice or synthesis of new monomers with special functional groups. Yu *et al.*<sup>13</sup> prepared an NF membranes by the interfacial polymerization of a polymeric polyamine, poly(vinyl amine), with isophthaloyl chloride on a polysulfone

supporting membrane. Tang *et al.*<sup>14</sup> fabricated an NF membrane by the interfacial polymerization of triethanolamine and trimethylolpropane triisocyanate (TMC) on a polysulfone supporting membrane. Zhang *et al.*<sup>15</sup> selected a natural tannic acid as the aqueous phase monomer to prepare NF on a poly(ether sulfone) (PES) supporting membrane. Other commonly used aqueous monomers include phenylene diamine-4-methyl,<sup>16</sup> hexafluoroalcohol phenylene diamine,<sup>17</sup> 3,5-diaminobenzoic acid,<sup>10</sup> 2,5-bis(4-amino-2-trifluoromethyl phenoxy)benzene sulfonic acid,<sup>18</sup> 4,4-bis(4-amino-2-trifluoromethylphenoxy) biphenyl-4,4-disulfonic acid,<sup>18</sup> and disulfonated bis[4-(3-aminophenoxy) phenyl] sulfone.<sup>19</sup> However, the use of macrocyclic polyamines as monomers to prepare NF membranes via interfacial polymerization has not been reported yet. Macrocyclic polyamine, which contains multiple amino groups, is a new type of total nitrogen crown ether. This compound exhibits the common properties and function of molecular recognition and good hydrophilicity because of its strong electrostatic charge and large pore size. These properties of macrocyclic polyamine are useful for preparing a polyamide membrane with good hydrophilicity.

In this study, thin-film composite NF membranes were prepared by interfacial polymerization with the aqueous monomer cyclen (a macrocyclic polyamine) and the organic monomer TMC. Additionally, silica sol dissolved in the aqueous phase was introduced as an additive during the interfacial polymerization process, in which SiO<sub>2</sub> nanoparticles were used to increase the water flux. In comparison to other aqueous monomers, such as polyethylenimine,<sup>20</sup> 2,2'-bis(1-hydroxyl-1-trifluoromethyl-2,2,2-trifluoroethyl)-4,4'-methylenedianiline,<sup>21</sup> and 4-aminobenzoyl piperazine,<sup>22</sup> the rejection of our membrane for Na<sub>2</sub>SO<sub>4</sub> was higher, or the membrane's water flux and hydrophilicity were all improved; this was due to the fact that our monomer contained multiple amino groups at the macrocycle.

## EXPERIMENTAL

### Materials

A PES UF membrane with an MWCO of 50,000 Da was fabricated in our laboratory. TMC (purity > 98%) was purchased from Qingdao Ocean Chemical Co. We synthesized cyclen [purity > 98.5%, as measured by gas chromatography/mass spectrometry (GC-MS)].<sup>22</sup> Silica sol (*m*SiO<sub>2</sub>·*n*H<sub>2</sub>O, radius < 10 nm) was supplied by Zhejiang Yuda Chemical Industry Co. Other reagents were purchased from Sinopharm Chemical Reagent Co.; these were of analytical-grade purity without further purification.

### Synthesis of the Aqueous Monomer Cyclen

The synthesis route of the aqueous monomer cyclen is shown in Figure 1. The reaction process was as follows. First, a solution of linear triethylene tetraamine (14.8 g, 0.1 mol) was added to *N,N*-dimethyl formamide dimethyl acetal (23.8 g, 0.2 mol) and stirred. The solution was refluxed for 2 h. Then, the reaction mixture was dried *in vacuo*. The resulting off-white solid was recrystallized from tetrahydrofuran, whereas the resulting white solid was filtered under a blanket of nitrogen and isolated at an 85% yield (14.2 g, 0.09 mol). Second, a 0.5-L four-necked, round-bottomed flask equipped with a mechanical stirrer, a thermometer, and a nitrogen inlet was charged with 0.15 L of

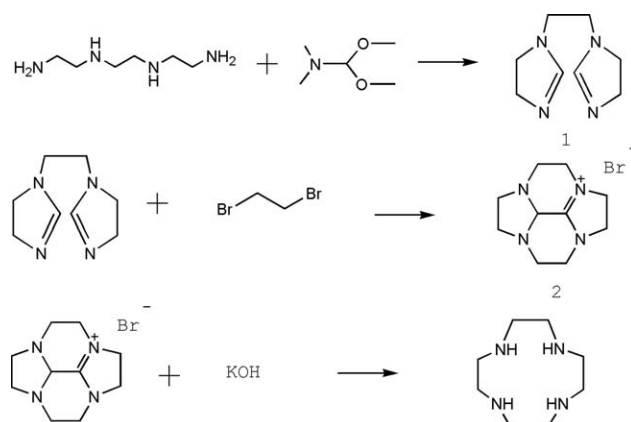
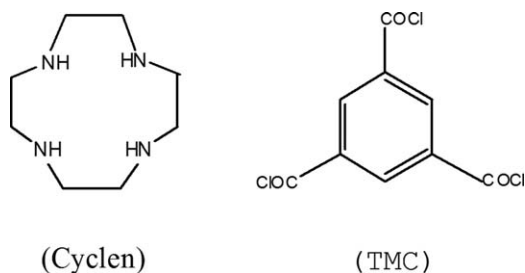


Figure 1. Synthesis route for the aqueous monomer cyclen.

acetonitrile, 1,1'-ethylenedi-2-imidazoline (16.6 g, 0.1 mol), 1,2-dibromoethane (26.3 g, 0.14 mol), and K<sub>2</sub>CO<sub>3</sub> (13.7 g, 0.1 mol). The mixed solution was then heated to reflux with constant stirring. After 3 h of refluxing, K<sub>2</sub>CO<sub>3</sub> was filtered, and the filtrate was dried *in vacuo*. Typically, the bromine salt (2) was removed from water without purification and carried on to the hydrolysis step. However, the pure salt form of 2 could be isolated through the rinsing of the crude solid with a minimal amount of cold acetonitrile followed by filtration under nitrogen; this yielded a pale yellow solid weighing 11.8 g (0.07 mmol) at a 70% yield. Finally, the bromine salt (2, 27.5 g, 0.1 mol) was dissolved in water to achieve a total volume of 80 mL and then added dropwise to a refluxing solution of 60 mL of caustic solution (KOH equivalent, 56 g, 1.0 mol). The caustic solution was heated for another 2 h after the addition of 2. The aqueous caustic solution was gravity-filtered while hot. The filtrate was then concentrated (*in vacuo*) until crystalline cyclen was observed in the solution. After the mixture was cooled to ambient temperature, cyclen was filtered, and the precipitation process was repeated until no further crystallization occurred. The final aqueous filtrate was dried *in vacuo*, and the remaining cyclen was removed through extraction of the solid residue with hot toluene. The overall yield of cyclen was 88% (15.1 g, 0.09 mol). The successful synthesis of cyclen was proven by <sup>1</sup>H-NMR and GC-MS.

### Fabrication of the Composite Membrane

The NF membranes were prepared by the interfacial polymerization technique of cyclen and TMC on a PES supporting membrane. The chemical structure of the aqueous monomer is shown in Figure 2. First, the UF support membrane was rinsed with the deionized water and then clamped between two Polytetrafluoroethylene (PTFE) frameworks 0.6 cm high with an inside diameter of 8 cm in an assembly clean room. The aqueous phase solution was prepared: cyclen and silica sol were dissolved in the deionized water, whereas the organic phase solution was composed of TMC in *n*-hexane. An aqueous phase solution was poured on the top surface of the PES UF membrane and allowed to sit for 5 min at ambient temperature. The concentration of cyclen in the aqueous solution was varied from 0.2 to 1.5 w/v. Excess monomer on the membrane surface was



**Figure 2.** Chemical structures of the monomers used.

drained. Afterward, the organic phase prepared by the mixture of the monomer TMC in *n*-hexane was poured onto the top surface of the PES UF membrane. The concentration of TMC in the organic solution was varied from 0.05 to 0.25 w/v. After a predetermined time for interfacial polymerization, the excess organic solution was poured off, and the membrane was heated at 60°C for several minutes to polymerize further. The final membrane was washed with the deionized water and kept in a 1% NaHSO<sub>3</sub> solution.

### Membrane Characterization

**Attenuated Total Reflectance (ATR)/Infrared (IR) Analysis.** ATR-IR (Nicolet, Magna-IR 550) was characterized by the chemical alteration of the NF membrane surface. For the NF membrane's ATR-IR analysis, an Irtran crystal at a 45° angle of incidence was used. The measured wave-number range was 4000–500 cm<sup>-1</sup>.

**Energy-Dispersive Spectrometry (EDS) and Scanning Electron Microscopy (SEM) Analysis.** EDS (JEOL JSM-6306LV) was used to determine the concentration of SiO<sub>2</sub> in the membrane skin layer. The morphologies of the cross sections of the NF membranes were observed with SEM (Hitachi S-3400N II) with a magnification of 50,000×.

**Atomic Force Microscopy (AFM) Analysis.** AFM (Veeco, NanoScopeIII a Multimode AFM) was used to analyze the surface morphology and roughness of the prepared membranes. The membrane surfaces were imaged at a scan size of 5 × 5 μm<sup>2</sup>. We obtained the membrane surface roughness in terms of the root mean square.

**Contact Angle Measurement.** A contact angle measurement instrument (JC2000D, PowerEach, China) was used to determine the water contact angle of the NF membranes.

### NF Performance Testing

The performances of the prepared membranes were tested by a batch cross-flow stainless steel system. The active membrane surface area was around 38.5 cm<sup>2</sup>. To make sure the membrane was in the steady state, the NF membranes were soaked in deionized water for 4 h to eliminate NaHSO<sub>3</sub> and then prepressurized under 0.6 MPa for 1 h with deionized water before the water flux and salt rejection were measured. The pure water fluxes were determined by the measurement of the time taken to collect 10 mL of permeate; this followed the passage of an initial 30 mL of permeate volume. The solutes [Mg(NO<sub>3</sub>)<sub>2</sub>, MgSO<sub>4</sub>, NaSO<sub>4</sub>, NaCl, PEG600, and PEG1000] were measured

at a 2000-ppm concentration, a pressure of 0.6 MPa, a temperature of 25 ± 0.5°C, and a pH of 7.0. The pure water flux was determined in an independent experiment at 0.6 MPa and 7.0 pH. The water fluxes and solution rejections obtained were average values. The permeation flux (*F*) was calculated as follows:

$$F = \frac{V}{A \times t} \quad (1)$$

where *V* is the total volume of the permeated fluid passing through the membrane during the experiment, *A* is the active area of the membrane, and *t* is the time of operation for permeation.

The rejection (*R*) was calculated as follows:

$$R = 1 - C_p / C_f \quad (2)$$

where *C<sub>p</sub>* and *C<sub>f</sub>* are the concentrations of the permeate and the feed solution, respectively, which were determined by a sodium conductivity meter (DDS-11A, Shanghai Leici Instrumental Plant).

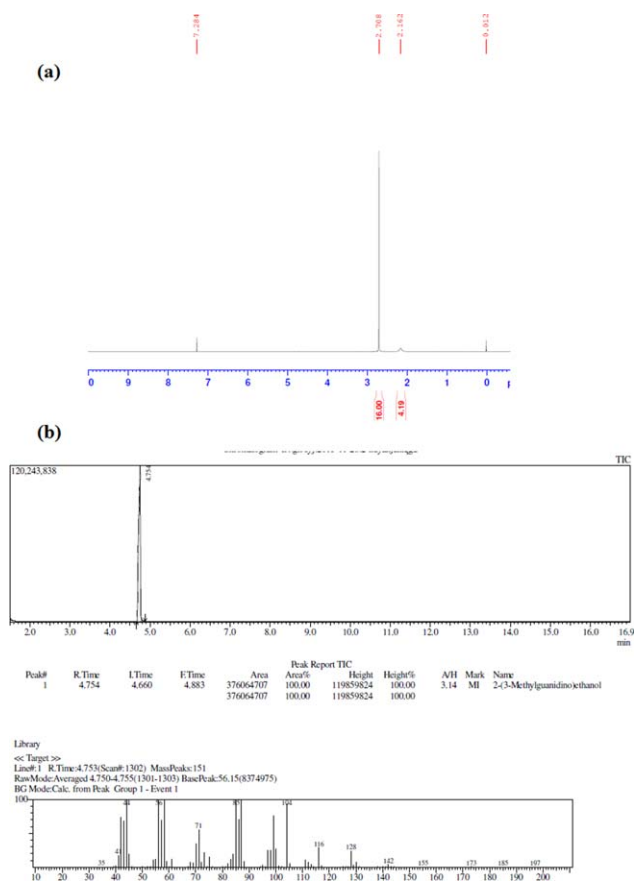


**Figure 3.** (a) <sup>1</sup>H-NMR and (b) GC-MS spectra of cyclen. [Color figure can be viewed in the online issue, which is available at [www.interscience.wiley.com](http://www.interscience.wiley.com).]

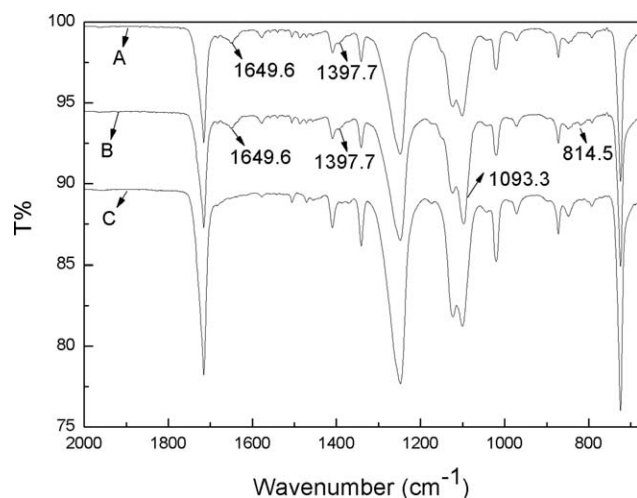


**Figure 4.** ATR-IR spectra of (a) the polycyclenamide NF membrane, (b) the silica sol/polycyclenamide NF membrane, and (c) the PES supporting membrane.

## RESULTS AND DISCUSSION

### <sup>1</sup>H-NMR and GC-MS of Cyclen

The synthesized cyclen was analyzed by <sup>1</sup>H-NMR and GC-MS (Figure 3). The following results were obtained:

<sup>1</sup>H-NMR (CDCl<sub>3</sub>) δ 2.71 (m, 16H), 2.16 (m, 4H) ppm. MS *m/e* 174 (*M* + 1): 173 (2), 128 (8), 104 (45), 85 (100), 56 (80). GC (100%). These values demonstrate that pure cyclen was successfully synthesized.<sup>22,23</sup>

### Structure and Morphology of the NF Membranes

**Fourier Transform Infrared Spectroscopy-ATR of the NF Membranes.** The chemical structures of the skin layers of the NF membranes evidently varied (Figure 4). Compared with the PES UF membrane, the Fourier transform infrared spectrum of the polycyclenamide NF membrane clearly presented the characteristic bands of amides I (C=O stretch) and II (C-N stretch) at 1649.6 and 1397.7 cm<sup>-1</sup>, respectively.<sup>24</sup> The peaks confirmed that polymerization occurred between the cyclen and TMC monomers. The active skin layer of the NF membrane was polyamide, which contained amide groups.

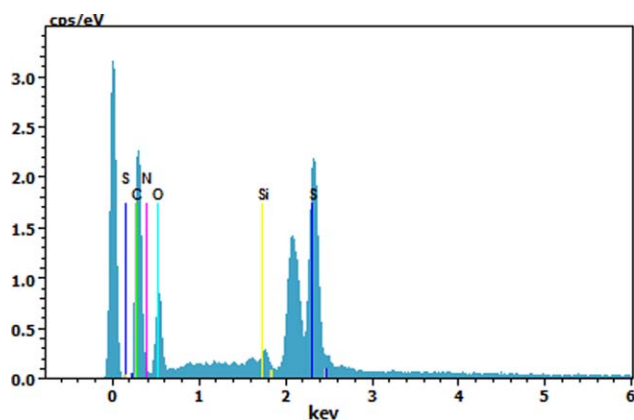


**Figure 5.** EDS spectrum of the silica sol/polycyclenamide NF membrane. [Color figure can be viewed in the online issue, which is available at [www.interscience.wiley.com](http://www.interscience.wiley.com).]

**Table I.** Relative Elemental Contents of the Silica Sol/Polycyclenamide NF Membrane

Element	wt %	atom %	Error (%)
C	28.65	35.35	9.4
N	16.13	17.07	6.3
O	47.46	43.96	15.9
Si	0.53	0.28	0.1
S	7.22	3.34	0.3

**EDS of the NF Membranes.** To further explore the silica sol content on the surface of the NF membrane, the EDS spectrum, and the elemental contents are presented in Figures 5 and Table I, respectively. The EDS spectrum exhibited an Si peak at 1.76keV. Meanwhile, the Si content was up to 0.53 wt %. Therefore, the skin layer of the membrane contained silica nanoparticles.

**SEM and AFM Images of NF Membranes.** Figure 6 shows the top surfaces and cross-sectional morphologies of the supporting membrane, polycyclenamide NF membrane, and silica sol/polycyclenamide NF membrane. It was clear that the polycyclenamide NF membrane took on a composite structure, namely, a thin and dense active function layer existing on the porous PES supporting membrane, and the addition of silica sol resulted in an increase in roughness in the skin layer of the resulting membrane. The AFM surface analysis of the supporting membrane and composite membranes was a further step for studying the morphological roughness of the NF membrane. As shown in Figure 7, the root mean square values of various membranes were as follows: PES supporting membrane = 12.7 nm, polycyclenamide NF membrane = 21.8 nm, and silica sol/polycyclenamide NF membrane = 46.4 nm. These values indicate that a rougher surface resulted from the addition of silica sol. As we all know, the sizes of silica sol were less than 10 nm. However, the size protuberances were obtained from the AFM images to be 100 nm; this may have been due to the fact that the silica particles were aggregated to a certain extent.

### Effects of the Preparation Conditions on the Performances of the NF Membranes

**TMC Concentration.** The monomer concentrations in the organic phases played a significant role in the preparation of the NF membranes by interfacial polymerization.<sup>25</sup> The effects of the TMC concentration in the organic phase were investigated in this study to optimize the performances of the NF membranes. In Figure 8, the experimental conditions were as follows: cyclen concentration = 1.0% w/v, reaction time = 15 s, and curing temperature for 15 min = 60°C. With increasing TMC concentration, the water fluxes sharply decreased from 72.8 to 17.8 L m<sup>-2</sup> h<sup>-1</sup>. However, the rejection increased when the TMC concentration increased from 0.05 to 0.10% w/v. When the TMC concentration exceeded 0.10% w/v, the rejection and water flux of NF membrane changed slightly. The rejection and water flux behavior of the membranes with TMC concentration may have been due to the morphology and thickness of the active layer. A low TMC concentration results in the lower polymerization rate, and the polyamide skin layer was

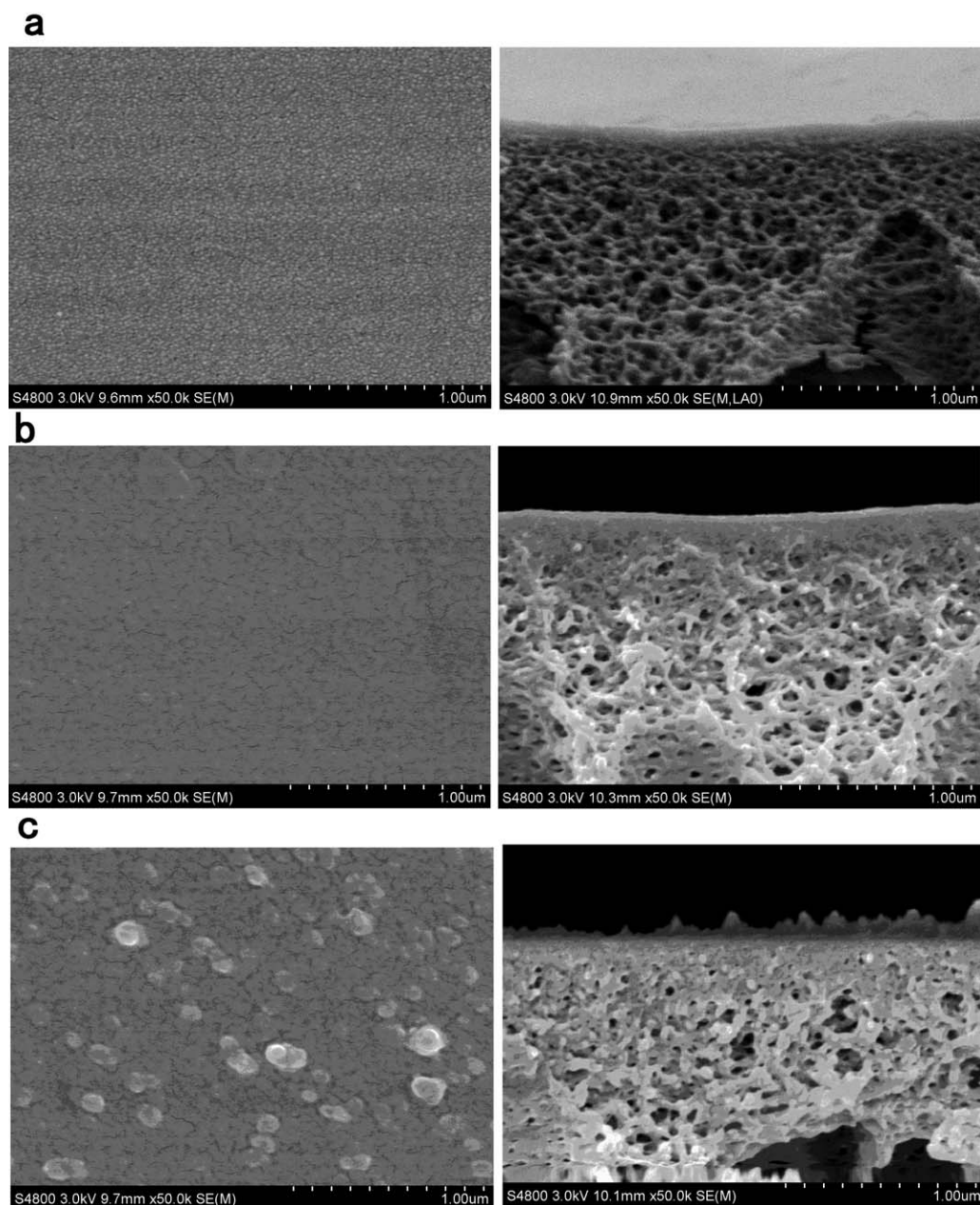


**Figure 6.** SEM images of the (a) supporting membrane, (b) polycyclenamide NF membrane, and (c) silica sol/polycyclenamide NF membrane (left, surface; right, cross section).

formed by a low-molecular-weight polymer. This characteristic reduced the salt rejection and increased the water flux. The high salt rejection and low water flux at a high TMC concentration were the consequences of the formation of a somewhat thicker and more compact polyamide skin layer because of the faster polymerization rate. A further increase in the TMC concentration after a certain concentration tended to have almost no further effect on the rate of polymerization. Thus, 0.10% w/v was used as the optimum TMC concentration to prepare the NF membranes.

**Cyclen Concentration.** The effects of cyclen aqueous solution concentration on the performance of the polycyclenamide

composite membrane are presented in Figure 9. The water flux decreased when the cyclen concentration increased from 0.2 to 2.0% w/v. At the same time, the salt rejection sharply increased and then leveled off after the cyclen concentration exceeded 1.0% w/v. The observed water flux and salt separation behavior of the membrane with cyclen concentration could be explained in terms of the thickness and morphology of the membranes. At a lower concentration, the polymerization was expected to proceed more slowly. This phenomenon resulted in the formation of a thin and loose polyamide skin layer with a lower salt rejection and higher water flux. With increasing cyclen concentration, the polymerization rate increased; this led to the formation of a somewhat thicker and

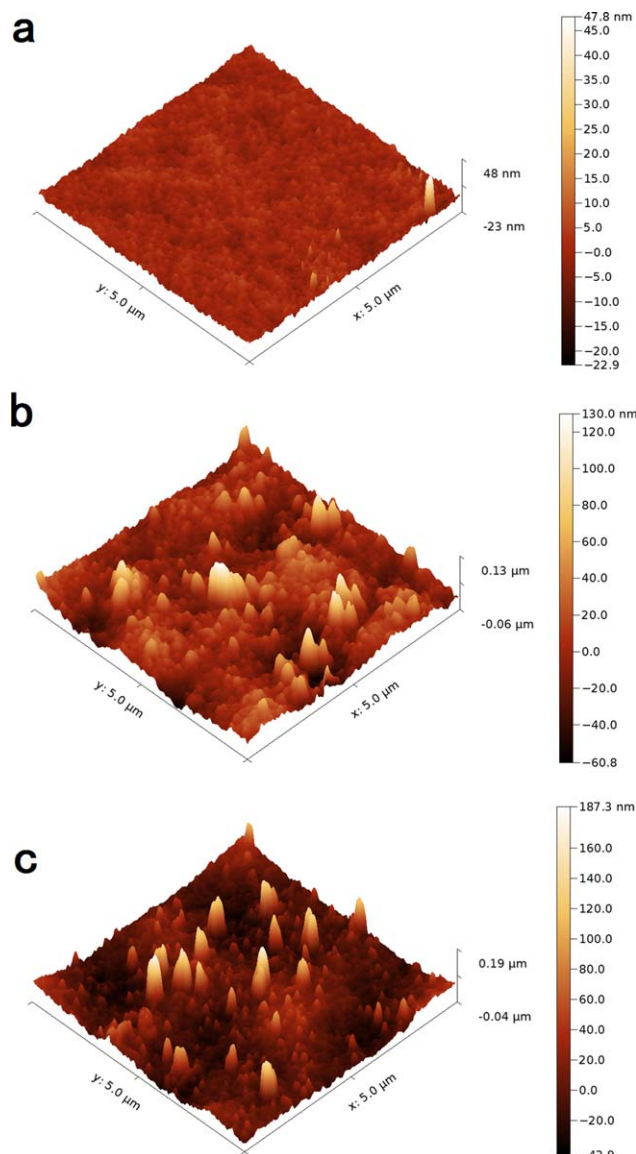


**Figure 7.** AFM images of the top surface morphologies of the (a) PES supporting membrane, (b) polycyclenamide NF membrane, and (c) silica sol/polycyclenamide NF membrane. [Color figure can be viewed in the online issue, which is available at [www.interscience.wiley.com](http://www.interscience.wiley.com).]

more compact network polycyclenamide skin layer. Hence, the salt rejection increased, and the water flux decreased. The interfacial polymerization speed was also influenced by the aqueous monomer diffusion rate; this also indicated the presence of an optimum concentration of reactants to obtain polymer membranes with excellent performance. Therefore, 1.0% w/v was used as the optimum cyclen concentration to prepare the NF membranes.

**Reaction Time.** The effect of the reaction time on the membrane performance is shown in Figure 10. The membrane rejection increased substantially as the reaction time increased from 10 to 15 s and then increased slightly from 15 to 45 s. At the same time, the membrane flux decreased quickly from 10 to

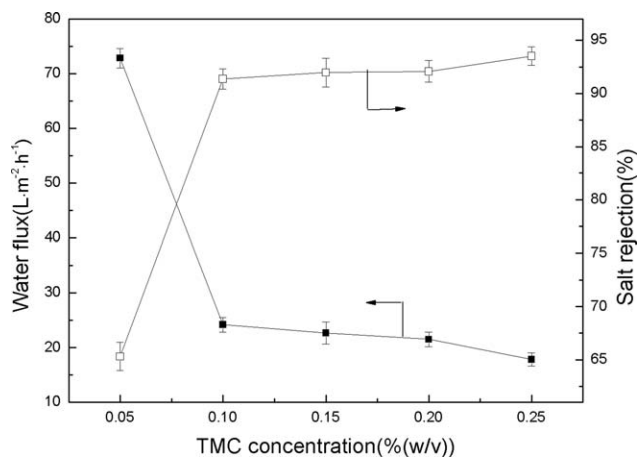


**Figure 8.** Effect of the TMC concentration on the salt rejection and water flux of the polycyclenamide NF membrane tested in a 2000-ppm  $\text{Na}_2\text{SO}_4$  aqueous solution at 0.6 MPa, 25°C, and pH 7.0.

15 s and then decreased slightly from 20 to 45 s. However, the flux increased from 15 to 20 s. The higher salt rejection and lower pure water flux may have resulted from the formation of a dense layer fabricated on the membrane surface; this was crosslinked between cyclen and TMC. Furthermore, the cross-linking reaction continued as time increased. When the reaction time was prolonged over 20 s, the formed active layer already changed the reaction barrier; this prevented monomers from diffusing to the reaction zone and led to a defective crosslinking structure. In the following study, NF membranes were fabricated under 20 s in reaction time.

**Curing Time.** To investigate the effect of the curing time on the water flux and salt rejection, a series of NF membranes were prepared under different curing times from 0 to 20 min at 60°C.<sup>26</sup> With increasing curing time from 0 to 15 min, the  $\text{Na}_2\text{SO}_4$  rejection increased from 79.1 to 94.1%, and the water flux decreased from 38.0 to 24.2  $\text{L m}^{-2} \text{h}^{-1}$  (Figure 11). However, with increasing curing time, the water flux increased, and the rejection of  $\text{Na}_2\text{SO}_4$  decreased. This behavior may have been

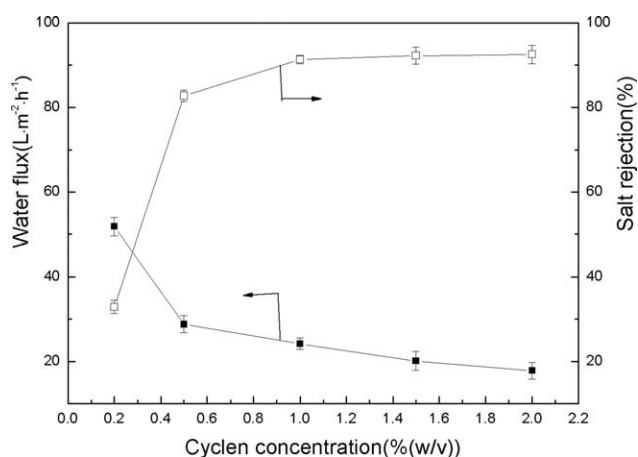


**Figure 9.** Effect of the cyclen concentration on the salt rejection and water flux of the polycyclenamide NF membrane tested in a 2000-ppm  $\text{Na}_2\text{SO}_4$  aqueous solution at 0.6 MPa, 25°C, and pH 7.0.

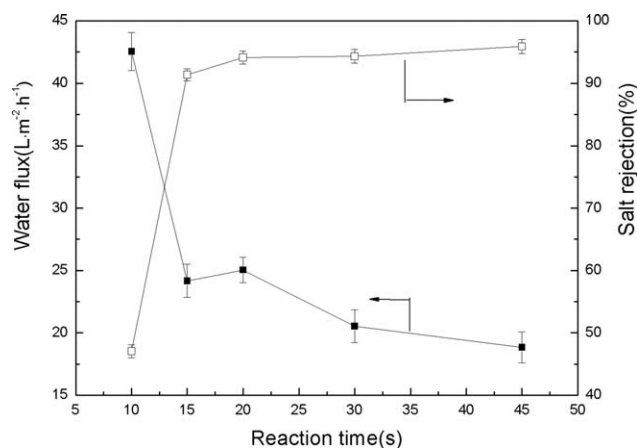


**Figure 10.** Effect of the reaction time on the salt rejection and water flux of the polycyclenamide NF membrane tested in a 2000-ppm  $\text{Na}_2\text{SO}_4$  aqueous solution at 0.6 MPa, 25°C, and pH 7.0.

due to a denser skin layer as the curing time increased at the beginning. A further increase in the curing time changed the structure of the membrane surface. With a gradual increase in time, the polymer started to contract, and the pores became larger; this led to an increased flux and reduced rejection. Therefore, the proper curing time had to be controlled at 15 min to attain a higher rejection.

**Silica Sol Concentration of the Aqueous Solution.** To further optimize membrane performance, the NF membranes were prepared by the interfacial polymerization of TMC with a mixture of cyclen and silica sol concentration on water flux and rejection of the NF membrane under the following conditions: 1.0% w/v cyclen and a certain concentration of silica sol in the aqueous phase, 0.10% w/v TMC in the organic phase, reaction time = 20 s, and curing temperature at 60°C = 15 min. Figure 12 shows the performance of the NF membranes prepared with different concentrations of silica sol. In this experiment, the water flux increased substantially, and the rejection decreased when the silica sol concentration was increased from 0 to 0.10% w/v. However, the rejection decreased substantially when the

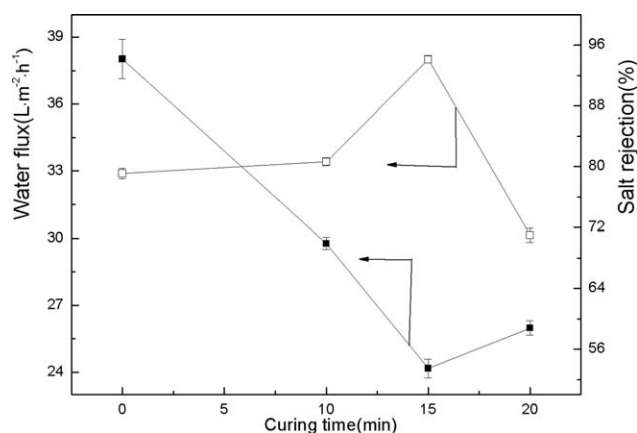


**Figure 11.** Effect of the curing time on the salt rejection and water flux of the polycyclenamide NF membrane tested in a 2000-ppm  $\text{Na}_2\text{SO}_4$  aqueous solution at 0.6 MPa, 25°C, and pH 7.0.

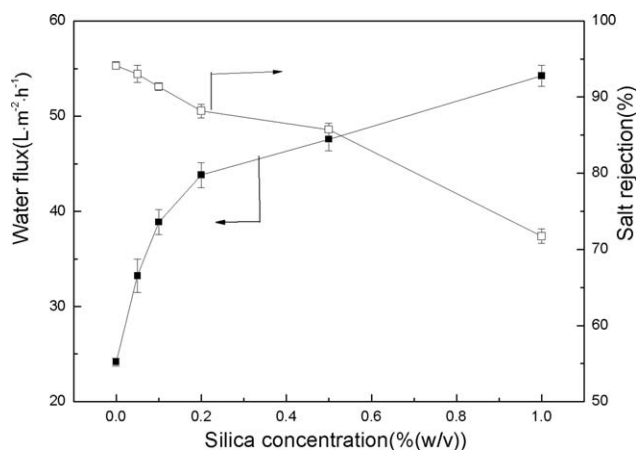


**Figure 12.** Effect of the silica sol concentration on the salt rejection and water flux of the resulting NF membrane tested in a 2000-ppm  $\text{Na}_2\text{SO}_4$  aqueous solution at 0.6 MPa, 25°C, and pH 7.0.

silica sol concentration increased slightly, and the water flux increased slightly. Considering both the good salt rejection and high water permeability, the 0.10% w/v silica sol concentration was optimum. This result was attributed to the fact that silica sol was dispersed on the supporting membrane surface, and the surface roughness increased with increasing silica sol concentration. In addition, the hydrophilicity of the NF membrane was improved by the incorporation of silica; this increased the water permeability.<sup>27,28</sup> This phenomenon was attributed to the numerous silanol or hydroxyl groups that covered the silica surface; this improved the hydrophilicity of the membrane. Such a phenomenon fit well with the result of the contact angle measurement (shown later in Figure 15). When the silica sol concentration was further increased, the water flux increased, whereas the salt rejection decreased substantially. These results were mainly attributed to the significant effects of interfacial polymerization by silica nanoparticles; this led to a low degree of polymerization of the active layer.<sup>29</sup>

**Operating Pressure.** The effect of the operating pressure on the polycyclenamide NF membrane performance is shown in Figure

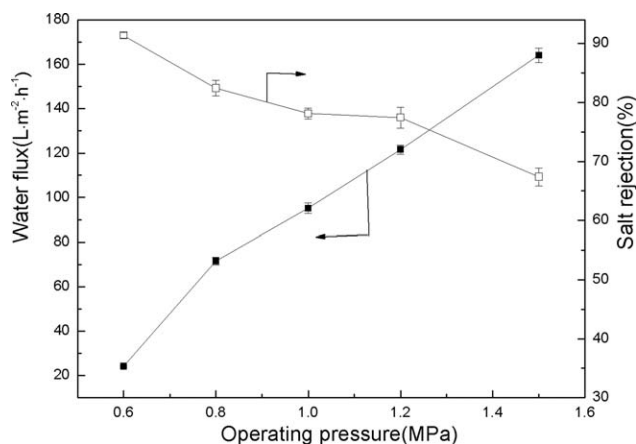


**Figure 13.** Effect of the operating pressure on the performance of the polycyclenamide NF membrane tested in a 2000-ppm  $\text{Na}_2\text{SO}_4$  aqueous solution at 25°C and pH 7.0.

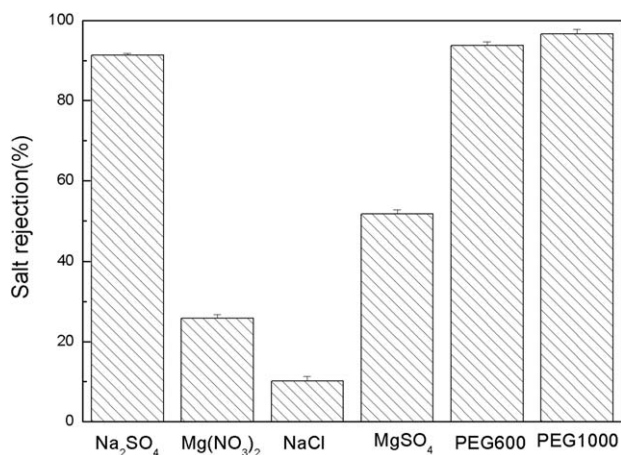


**Figure 14.** Rejection of different types of salts and organic compounds by the silica/polycyclenamide NF membrane.

13. When the operating pressure was increased from 0.6 to 1.5 MPa, the salt rejection decreased from 91.4 to 61.4%, and the water flux of the membrane increased quickly from 24.2 to 164.2 L m<sup>-2</sup> h<sup>-1</sup>. These trends were similar to those reported by Sun *et al.*<sup>2</sup> The water flux of the membrane increased with increasing operating pressure; this could be explained by the Spiegler–Kedem model:<sup>30</sup>

$$J_v = L_p(\Delta P - \sigma \Delta \pi)$$

where  $J_v$  is the water flux,  $L_p$  is the water permeability,  $\Delta P$  is the transmembrane pressure,  $\sigma$  is the reflection factor of the membrane, and  $\Delta \pi$  is the osmosis pressure.

The membrane we prepared was negatively charged; this was proven as discussed in the next section. Therefore, the rejection was mainly determined by Donnan exclusion. However, the weaker rejection was affected by the operating pressure. So, the salt rejection decreased slightly with increasing operating pressure.

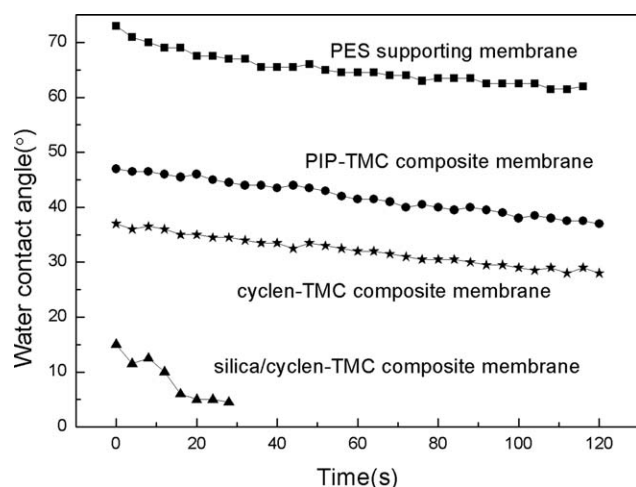


**Figure 15.** Dynamic water contact angles of the membranes. PIP: Piperazine.

### Rejection of Different Inorganic Electrolytes and Poly(ethylene glycol)s of the NF Membranes

To characterize the charge performance of the membrane, the salt rejection of the silica sol/polycyclenamide NF membrane was investigated, and the surface charge was evaluated according to the order of salt rejection. In the experiment, four kinds of salt solutions [Na<sub>2</sub>SO<sub>4</sub>, Mg(NO<sub>3</sub>)<sub>2</sub>, NaCl, and MgSO<sub>4</sub>] were used at a concentration of 2000 mg/L and a filtrate pressure of 0.6 MPa. The order of salt rejection of the NF membrane was Na<sub>2</sub>SO<sub>4</sub> > MgSO<sub>4</sub> > Mg(NO<sub>3</sub>)<sub>2</sub> > NaCl; this indicated that the prepared novel NF membrane tended to be a negatively charged membrane.<sup>13</sup> At the same time, the rejections of PEG600 and PEG1000 for the silica sol/polycyclenamide NF membrane were measured (Figure 14). Generally, the MWCO is the molecular weight of an organic substance with a retention of 90%. Therefore, the MWCO of NF membrane was under 600 Da.

### Dynamic Water Contact Angles of the NF Membranes

The dynamic water contact angle data of all of the membranes were characterized by the curve of the water drop angle versus the contact time (Figure 15). Compared with the PES supporting membrane, the hydrophilicity of the polycyclenamide NF membrane improved well because of the presence of several hydrophilic groups, including amine, carboxyl, and acylamino. The hydrophilicity of the silica sol/polycyclenamide NF membrane was evidently superior. This characteristic was attributed to the rougher surface or the hydroxyl groups on the surface of the silica. Moreover, the hydrophilicity of the polycyclenamide NF membrane was also superior to that of the polypiperazine–amide NF membrane, which was prepared under similar preparation conditions.

### CONCLUSIONS

A novel NF membrane was successfully prepared from cyclen and TMC through interfacial polymerization on the PES supporting membrane. The optimal preparation parameters for the polycyclenamide NF membrane were as follows: TMC concentration = 0.10% w/v, cyclen concentration = 1.0% w/v, immersion time in the aqueous phase = 5 min, reaction time = 20 s, and curing temperature at 60°C = 15 min. The effects of the operating conditions on the performance of the NF membrane were also discussed. The NF membrane exhibited an Na<sub>2</sub>SO<sub>4</sub> rejection of 94.1% and water flux of 24.2 L·m<sup>-2</sup>·h<sup>-1</sup> at an operating pressure of 0.6 MPa. After the addition of silica sol in the aqueous phase (silica sol concentration = 0.10% w/v), the Na<sub>2</sub>SO<sub>4</sub> rejection of the membrane changed slightly, but the water flux increased from 24.2 L·m<sup>-2</sup>·h<sup>-1</sup> (25°C, 0.6 MPa) up to 38.9 L·m<sup>-2</sup>·h<sup>-1</sup> (25°C, 0.6 MPa); this was nearly 60.7% higher than that of polycyclenamide NF membrane. The silica/polycyclenamide NF membrane exhibited excellent hydrophilicity. The rejections of the resulting NF membranes for Na<sub>2</sub>SO<sub>4</sub>, MgSO<sub>4</sub>, Mg(NO<sub>3</sub>)<sub>2</sub>, NaCl, PEG600, and PEG1000 were 91.4, 51.7, 25.8, 10.1, 93.8, and 96.7%, respectively. The orders of the different salt rejections were used to explain the fabricated NF membrane with typical characteristics for negatively charged membranes.



## ACKNOWLEDGMENTS

The authors are thankful for financial support received from the National Natural Science Foundation of China (contract grant number 51172144), the Shanghai Union Program (contract grant number LM201249), the Key Technology R&D Program of the Shanghai Committee of Science and Technology in China (contract grant numbers 13521102000 and 14231201503), the 2013 Special Project of the Development and Industrialization of New Materials of the National Development and Reform Commission in China (contract grant number 20132548), and the Key Technology R&D Program of the Jiangsu Committee of Science and Technology in China (contract grant number BE2013031).

## REFERENCES

1. Cheng, Z.; Wu, C.; Yang, W.; Xu, T. *J. Membr. Sci.* **2010**, *358*, 93.
2. Sun, H.; Chen, G.; Huang, R.; Gao, C. *J. Membr. Sci.* **2007**, *297*, 51.
3. Miao, J.; Chen, G.; Gao, C.; Lin, C.; Wang, D.; Sun, M. *J. Membr. Sci.* **2006**, *280*, 478.
4. Li, L.; Zhang, S.; Zhang, X. *J. Membr. Sci.* **2009**, *335*, 133.
5. Li, X.; Cao, Y.; Yu, H.; Kang, G.; Jie, X.; Liu, Z.; Yuan, Q. *J. Membr. Sci.* **2014**, *466*, 82.
6. Jeong, B.-H.; Hoek, E. M. V.; Yan, Y.; Subramani, A.; Huang, X.; Hurwitz, G.; Ghosh, A. K.; Jawor, A. *J. Membr. Sci.* **2007**, *294*, 1.
7. Korikov, A. P.; Kosaraju, P. B.; Sirkar, K. K. *J. Membr. Sci.* **2006**, *279*, 588.
8. Mohammad, A. W.; Hilal, N.; Abu Seman, M. N. *Desalination* **2003**, *158*, 73.
9. Razdan, U.; Kulkarni, S. S. *Desalination* **2004**, *161*, 25.
10. Zhan, S.; Yang, J.; Liu, Y.; Wang, N.; Dai, J.; Yu, H.; Gao, X.; Li, Y. *J. Colloid Interface Sci.* **2011**, *355*, 328.
11. Meihong, L.; Sanchuan, Y.; Yong, Z.; Congjie, G. *J. Membr. Sci.* **2008**, *310*, 289.
12. Ghosh, A. K.; Jeong, B.-H.; Huang, X.; Hoek, E. M. V. *J. Membr. Sci.* **2008**, *311*, 34.
13. Yu, S.; Ma, M.; Liu, J.; Tao, J.; Liu, M.; Gao, C. *J. Membr. Sci.* **2011**, *379*, 164.
14. Tang, B.; Huo, Z.; Wu, P. *J. Membr. Sci.* **2008**, *320*, 198.
15. Zhang, Y.; Su, Y.; Peng, J.; Zhao, X.; Liu, J.; Zhao, J.; Jiang, Z. *J. Membr. Sci.* **2013**, *429*, 235.
16. Yu, S.; Liu, M.; Lü, Z.; Zhou, Y.; Gao, C. *J. Membr. Sci.* **2009**, *344*, 155.
17. La, Y.-H.; Sooriyakumaran, R.; Miller, D. C.; Fujiwara, M.; Terui, Y.; Yamanaka, K.; McCloskey, B. D.; Freeman, B. D.; Allen, R. D. *J. Mater. Chem.* **2010**, *20*, 4615.
18. Liu, Y.; Zhang, S.; Zhou, Z.; Ren, J.; Geng, Z.; Luan, J.; Wang, G. *J. Membr. Sci.* **2012**, *394*, 218.
19. Xie, W.; Geise, G. M.; Freeman, B. D.; Lee, H.-S.; Byun, G.; McGrath, J. E. *J. Membr. Sci.* **2012**, *403*, 152.
20. Wu, D.-H.; Huang, Y.-F.; Yu, S.-C.; Darren, L.; Feng, X.-S. *J. Membr. Sci.* **2014**, *472*, 141.
21. Hu, D.; Xu, Z.-L.; Wei, Y.-M.; Cao, S.; Chen, W.-D.; Qian, X.-H. *Sep. Sci. Technol.* **2013**, *48*, 554.
22. Phillip, S. A.; Garry, E. K. *J. Org. Chem.* **2002**, *67*, 4081.
23. Jennifer, M. W.; Federica, G.; Louis, J. F.; Michael, P. B.; David, J. R.; Andrew, S. *Org. Biomol. Chem.* **2007**, *5*, 3651.
24. Vidal, B. C.; Mello, M. L. *Micron* **2011**, *42*, 283.
25. Chen, S.-H.; Chang, D.-J.; Liou, R.-M.; Hsu, C.-S.; Lin, S.-S. *J. Appl. Polym. Sci.* **2003**, *83*, 1112.
26. Gao, J.; Sun, S.-P.; Zhu, W.-P.; Chung, T.-S. *J. Membr. Sci.* **2014**, *452*, 300.
27. Wu, H.; Tang, B.; Wu, P. *J. Membr. Sci.* **2013**, *428*, 341.
28. Jadav, G. L.; Singh, P. S. *J. Membr. Sci.* **2009**, *328*, 257.
29. Lee, H. S.; Im, S. J.; Kim, J. H.; Kim, H. J.; Kim, J. P.; Min, B. R. *Desalination* **2008**, *219*, 48.
30. Spiegler, K. S.; Kedem, O. *Desalination* **1966**, *1*, 311.